

# Influence of the Attachment of Chromophores to a Polymer Chain on Their Twisted Intramolecular Charge-Transfer State in Dilute Solution

Agnieszka Bajorek and Jerzy Pączkowski\*

Faculty of Chemical Technology and Engineering, University of Technology and Agriculture, Seminaryjna 3, 85-326 Bydgoszcz, Poland

Received March 18, 1997; Revised Manuscript Received October 27, 1997

**ABSTRACT:** Fluorescence from the initially excited singlet state (LE) and the twisted intramolecular charge-transfer (TICT) state of 4-(*N,N*-dimethylamino)benzoate (DMAB), 4-(*N,N*-diethylamino)benzoate (DEAB), 4-(*N*-pyrrolidino)benzoate (PYR), 4-(*N*-piperidino)benzoate (PIP), 4-(*N*-morpholino)benzoate (MOR), and 4-(*N*-2,6-dimethylmorpholino)benzoate (26DMM) were compared with the free and polystyrene-bound chromophores. The ground-state twisting of the donor with respect to the acceptor can have a large influence on the charge distribution. The polymeric chain can force a less planar geometry and cause a bathochromic shift and a broadening of the absorption band in the electronic absorption spectra. In the area of 350 nm the emission is assigned to the locally excited state (with a planar geometry) and the emission with  $\lambda_{\text{fl}}^{\text{max}}$  in the area of 450–520 nm to the TICT state (with a perpendicular conformation). Experimental results show (i) no polymeric chain effect in emission distribution for the DMAB molecule, (ii) a significant red edge effect (REE) for the PIP probe, (iii) a slight red edge effect for 26DMM, (iv) a specific blue edge effect (BEE) for PYR probe, and (v) a combination of REE and BEE for MOR. Adaptation of Grabowski's TICT hypothesis allows one to calculate the activation energy of TICT state formation, the backreaction TICT  $\rightarrow$  LE, and the thermally activated TICT fluorescence. The polymeric chain essentially does not change the activation energy ( $E_i$ ) for the thermally activated TICT state formation, indicating that the polymeric chain does not change the microscopic viscosity in the range affecting measurable changes in the TICT–LE equilibrium. The polymeric chain increases the gap between the lowest forbidden  $\nu_0$  vibrational state and less forbidden  $\nu_1$  vibrational state by 195–225  $\text{cm}^{-1}$  (0.6–2.4 kJ  $\text{mol}^{-1}$ ). Experimental results suggest that the polymer chain affects only the vibrational relaxation of tested molecules without any significant effect on the thermodynamics of the TICT and LE states equilibrium.

## Introduction

In polymeric systems changes in the fluorescence yield,<sup>1–4</sup> the position of fluorescence maximum,<sup>5,6</sup> changes in polarization,<sup>7,8</sup> and the efficiency of intermolecular excimer formation<sup>9–11</sup> have been related to the microscopic viscosity combining the effects of solvent and the relaxing chromophore to alter fluorescent properties. The difference between the microscopic and macroscopic viscosity, measured by viscosimetric techniques, was illustrated by Nishijama and co-workers,<sup>12,13</sup> who compared the depolarization of fluorescence, a measurement of microscopic viscosity, to the melt viscosity. It was deduced that the microscopic viscosity is related to the movement of the polymer segments of about molecular weight 2000, e.g., 60 ethylene units. It was shown that the microscopic viscosity changes linearly up to a certain degree of polymerization, reaching a plateau beyond that.

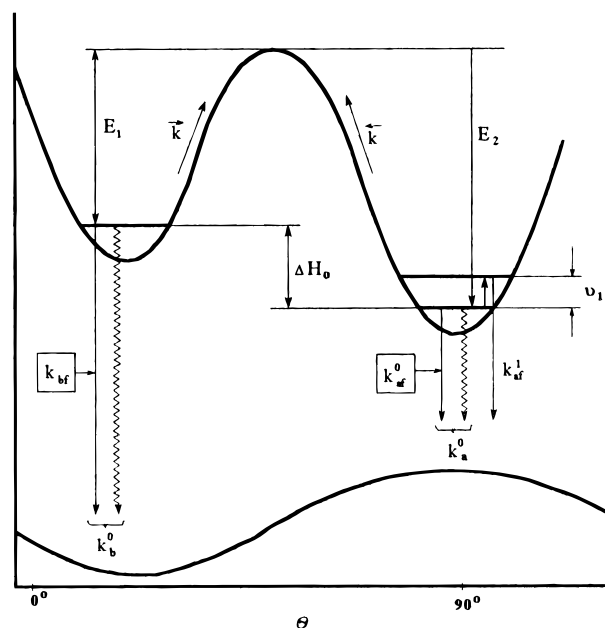
In a dilute polymer solution, the dynamical behavior of an isolated flexible chain may be characterized by a broad distribution of the relaxation times. Two limiting cases are of interest: In a poor solvent, in which the polymer segments effectively attract each other and the chain tends to contract, the environmental properties of the solution surrounding the relaxing fluorescent molecule attached to the chain might be more affected by the polymer chain. In a good solvent contacts between polymer chain segments are unfavorable and properties of the solvent cage surrounding the fluores-

cence probe are affected little by the polymer. For the description of the solute–solvent interaction in polymeric solutions one can adopt the Onsager<sup>14</sup> treatment of solute–solvent interaction applicable to molecules with a permanent dipole moment. Since the molecules in the electronically excited states are sensitive to the molecular environment, luminescence spectroscopy provides a powerful technique for monitoring the polymer structure and mobility. A number of studies have been reported on the use of excimer or exciplex formation in polymeric systems to examine the local segment mobility and the study of the microenvironment. More recently, fluorescence probes indicating the photoinduced intramolecular electron transfer process (PET) have been of more interest, especially for the monitoring of the rate of polymerization or physical processes occurring during and after polymerization.<sup>15,16</sup> All these applications of luminescence spectroscopy have been the subject of several reviews.<sup>17–20</sup>

The photoinduced intramolecular electron transfer (PET) is typical for aromatic systems with strong donor and acceptor substituents which often exhibit anomalous emission properties, e.g., a large Stokes shift or dual fluorescence in polar solvent. In rigid molecules an unusually large Stokes shift, which is explained by the increase of the excited-state dipole moment and the theory of solvent shift,<sup>21–24</sup> is observed. In flexible molecules, only one fluorescence band is found, possibly due to internal relaxation channels, which involve several kinds of rotations around molecular bonds.<sup>25–27</sup> Flexible systems are useful for the study of polymeric systems,<sup>1,7,25,28</sup> because of their high sensitivity to the

\* To whom correspondence should be addressed.

Scheme 1



viscosity and the polarity of surrounding solvent molecules.

It has been known for some time that a certain series of 4-(*N,N*-dimethylamino)benzonitriles<sup>29–31</sup> (DMABN) or 4-(*N,N*-dimethylamino)benzoates<sup>32</sup> (DMAB) exhibits a characteristic double fluorescence corresponding to the two kinds of singlet excited states (see Scheme 1).

According to the twisted intramolecular charge-transfer (TICT) hypothesis proposed by Grabowski and co-workers,<sup>33,34</sup> the short-wavelength (*b*<sup>\*</sup>) band is due to a coplanar molecule, while the long-wavelength (*a*<sup>\*</sup>) band originates from a molecule with a perpendicular conformation, which causes full charge separation. Thus, the fluorescence spectra of these molecules depend strongly not only on the solvent polarity but also on the medium viscosity,<sup>35,36</sup> and the molecules are expected to act as molecular probes.

For polymeric solution, the work of Hayashi and Tazuke,<sup>37,38</sup> illustrates the difference between the microscopic and macroscopic viscosity. It was shown that the relative intensities of the *a*<sup>\*</sup> and *b*<sup>\*</sup> bands are different for the free probe molecules and for the DMAB attached to the polymeric chain and that for the polymeric system below room temperature the ratio of the emission intensities of *a*<sup>\*</sup> and *b*<sup>\*</sup> bands is kinetically controlled, while in the monomeric analog an equilibrium has been reached. It was concluded that the twisting of the dimethylamino groups is strongly impeded when it is attached to the polymer, that the activation energy for the formation of the twisted form remains constant up to polymer concentration of 75 wt %, and that polymer side chains control the ground-state conformational distribution of the DBAB chromophore, as demonstrated by the red edge effect (REE) and by the broadening of the absorption spectra.

More recently, Zachariasse et al.<sup>39,40</sup> while studying properties of 4-(dialkylamino)benzonitriles (DMABN) noticed that the dual emission of these molecules can be explained assuming that the dual fluorescence results from a reversible intramolecular charge-transfer (ICT) reaction. From the initially excited singlet state (LE), species (CT) with a considerably larger dipole moment are produced. In toluene a strong dual fluo-

rescence was found at lower temperatures,<sup>39</sup> as well as an additional red-shifted CT emission in the fluorescence spectrum of DMABNs, which indicates that intramolecular charge transfer occurs at room temperature in 1,4-dioxane, benzene, and cyclohexane.<sup>40</sup>

In our studies, six 4-(*N,N*-dialkylamino)benzoates with varying "sizes" of "rotating" parts were used in order to probe the polymer chain influence on their spectroscopic properties.

## Experimental Section

**General Remarks.** Styrene, substrates for synthesis, and all solvents (spectroscopic grade) were purchased from Aldrich. Electronic absorption spectra were recorded with a UV-vis Varian Cary 3E spectrophotometer. The fluorescence spectra were obtained using a Hitachi F-4500 fluorescence spectrophotometer equipped with a homemade quartz Dewar flask allowing the fluorescence to be monitored at various temperatures. The fluorescence quantum yields were measured using *p*-terphenyl as the actinometer. <sup>1</sup>H-NMR spectra were obtained using a Varian Gemini 200 NMR spectrometer.

**Synthesis.** Polystyrenes labeled with 4-(*N,N*-dialkylamino)benzoate (poly-DMAB, poly-DEAB, poly-PYR, poly-PIP, poly-MOR, and poly-26DMM) groups were prepared by the sequence of reactions described in Scheme 2. Synthesis of polystyrene labeled by 4-(*N,N*-dimethyl(ethyl)amino)benzoate residues was described in our earlier paper.<sup>41</sup> The amount of sodium 4-(*N,N*-dialkylamino)benzoate used allowed one to attach statistically one probe molecule for 40 styrene units. The starting chloromethylated polystyrene was obtained by copolymerization of 3 mol of styrene and 1 mol of vinylbenzyl chloride (mixture of 60% meta and 40% para isomers). The resulting poly(styrene-vinylbenzyl chloride) contains 2.15 mmol g<sup>-1</sup> of CH<sub>2</sub>Cl groups.

Polystyrenes having 4-(*N,N*-dialkylamino)benzoate residue in a side chain were prepared starting from chloromethylated polystyrene modified by a 4-fluorobenzoate residue followed by reaction with a cyclic aliphatic amine to yield the final product, using the modified procedure given by Shur.<sup>38,42</sup>

**Polystyrenes Having PIP in a Side Chain.** A total of 4.7 g (10 mmol of -CH<sub>2</sub>Cl groups) of chloromethylated polystyrene was dissolved in 40 mL of dry DMF. To this solution were added 1 mmol (0.162 g) of sodium salt of 4-fluorobenzoic acid and 0.2 g of tetrabutylammonium bromide (TBAB) as a phase-transfer catalyst. The reaction mixture was stirred at 40–45 °C for 24 h. The resulting mixture was then cooled to room temperature, and the resulting polymer was precipitated in methanol and purified by repeated precipitation in methanol from CHCl<sub>3</sub> solution; 3.5 g of the resulting polymer was dissolved in 25 mL of dry DMF, and to the solution were added 0.34 g (4 mmol) of piperidine and 20 mL of DMSO. The reaction mixture was stirred at 100 °C for 24 h. The modified polymer was precipitated in methanol and was purified by repeated precipitation in methanol from a CHCl<sub>3</sub> solution.

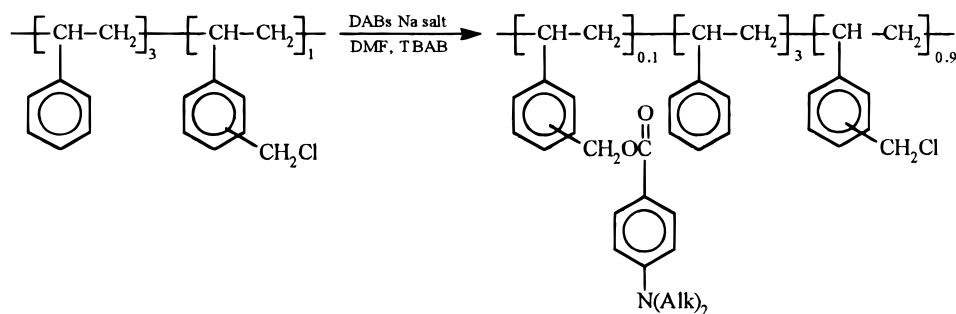
Polystyrenes labeled by 4-(*N*-morpholino)benzoate (poly-MOR), 4-(*N*-pyrrolidino)benzoate (poly-PYR), and 4-(*N*-2,6-dimethylmorpholino)benzoate (poly-26DMM) residues were prepared using similar procedures.

Butyl 4-(*N*-piperidino)benzoate (PIP) was prepared by using a sequence of reactions starting from 4-fluorobenzoic acid through butyl 4-fluorobenzoate to yield the final product, using a general procedure given by Shur.<sup>38,47</sup> Butyl 4-(*N*-morpholino)benzoate (MOR), butyl 4-(*N*-pyrrolidino)benzoate (PYR), and butyl 4-(*N*-2,6-dimethylmorpholino)benzoate (26DMM) were prepared by a similar procedure. Structures were confirmed from their NMR spectra.

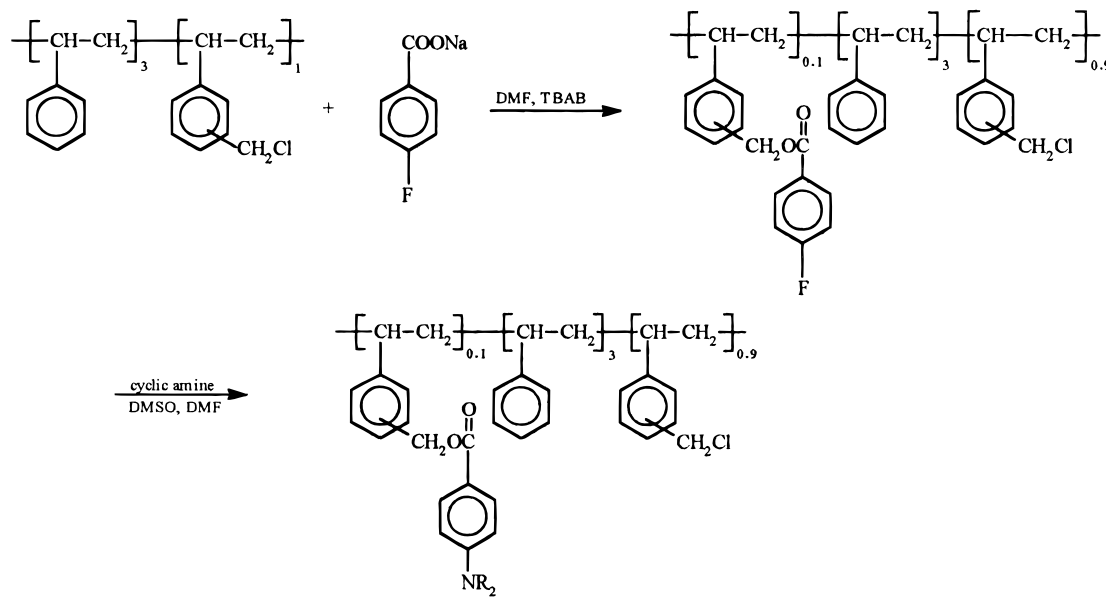
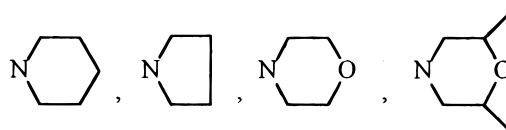
**1. Butyl 4-(*N*-morpholino)benzoate (MOR):** <sup>1</sup>H-NMR (CDCl<sub>3</sub>, ppm) 7.968, 7.923 (*J*<sub>ab</sub> = 9.0 Hz, 2H, Ph), 6.926, 6.881 (*J*<sub>ab</sub> = 9.0 Hz, 2H, Ph), 4.240–4.306 (t, 2H, C(O)O-CH<sub>2</sub>, butyl), 3.847–3.896 (t, 4H, CH<sub>2</sub>-O-CH<sub>2</sub>, morpholine), 3.254–3.303 (t, 4H, CH<sub>2</sub>-N-CH<sub>2</sub>, morpholine), 1.656–1.756 (m, 2H, CH<sub>2</sub>,

Scheme 2

a



b

where:  $R_2$ 

butyl), 1.404–1.503 (m, 2H,  $CH_2$ , butyl), 0.925–0.997 (t, 3H,  $CH_3$ -, butyl).

**2. Butyl 4-(*N,N*-diethylamino)benzoate (DEAB):**  $^1H$ -NMR ( $CDCl_3$ , ppm) 7.910–7.865 ( $J_{ab} = 9.0$  Hz, 2H, Ph), 6.650, 6.605 ( $J_{ab} = 9.0$  Hz, 2H, Ph), 4.221–4.286 (t, 2H,  $C(O)O-CH_2$ -, butyl), 3.346–3.451 (q, 4H,  $CH_2$ ,  $N(Et)_2$ ), 1.80 (m, 2H,  $CH_2$ -, butyl), 1.40 (m, 2H,  $CH_2$ , butyl), 1.146–1.217 (t, 6H,  $CH_3$ , ethyl), 0.922–0.994 (t, 3H,  $CH_3$ , butyl).

**3. Butyl 4-(*N*-piperidino)benzoate (PIP):**  $^1H$ -NMR ( $CDCl_3$ , ppm) 7.929, 7.884 ( $J_{ab} = 9.0$  Hz, 2H, Ph), 6.930, 6.885 ( $J_{ab} = 9.0$  Hz, 2H, Ph), 4.229–4.295 (t, 2H,  $C(O)O-CH_2$ , butyl), 3.294–3.321 (m, 4H,  $CH_2-N-CH_2$ -, piperidine), 1.650–1.700 (m, 8H,  $CH_2-CH_2$ , butyl, piperidine), 1.40–1.60 (m, 2H,  $CH_2$ , butyl), 0.922–0.995 (t, 3H, butyl).

**4. Butyl 4-(*N*-pyrrolidino)benzoate (PYR):**  $^1H$ -NMR ( $CDCl_3$ , ppm) 7.929, 7.884 ( $J_{ab} = 9.0$  Hz, 2H, Ph), 6.930, 6.885 ( $J_{ab} = 9.0$  Hz, 2H, Ph), 4.229–4.295 (t, 2H,  $C(O)O-CH_2$ -, butyl), 3.297–3.362 (t, 4H,  $CH_2-N-CH_2$ -, pyrrolidine), 1.985–2.050 (m, 4H,  $CH_2-CH_2$ , pyrrolidine), 1.6–1.7 (m, 2H,  $CH_2$ ,

butyl), 1.3–1.5 (m,  $CH_2$ , butyl), 0.914–0.986 (t, 3H,  $CH_3$ , butyl).

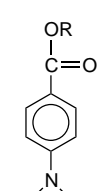
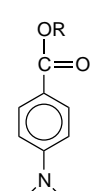
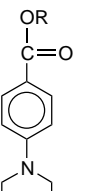
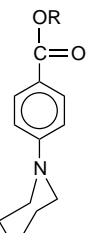
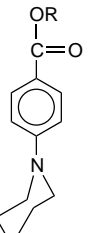
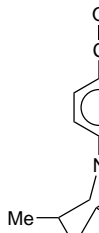
**5. Butyl 4-(*N*-2,6-dimethylmorpholino)benzoate (2,6DMM):**  $^1H$ -NMR ( $CDCl_3$ , ppm) 7.968, 7.923 ( $J_{ab} = 9.0$  Hz, 2H, Ph), 6.926, 6.881 ( $J_{ab} = 9.0$  Hz, 2H, Ph), 4.139–4.205 (t, 2H,  $C(O)O-CH_2$ , butyl), 3.439–3.495 (q, 2H, (2,6)-morpholine), 1.622–1.694 (m, 2H, butyl), 1.383–1.450 (m, 2H, butyl), 1.218–1.249 (d, 6H, methyl, morpholine), 0.895–0.968 (t, 3H, butyl).

## Results and Discussion

The structures of probes used in our study along with their basic photophysical properties are summarized in Table 1. Figure 1 shows the absorption spectra recorded for PIP and poly-PIP.

In dilute solution, the shape of the electronic absorption curve recorded for the polymeric system and for the monomeric model is almost identical, except for a slight

Table 1. Spectroscopic Characteristics of Tested Probes in THF Solution

molecule						
abbreviation	DMAB	DEAB	PYR	PIP	MOR	26DMM
monomer $\lambda_{\max}^A$ [nm]	307.2	311.6	312.0	306.4	300.0	301.0
$\epsilon_{\max}$	33900	31400	32800	24700	23000	17000
CT band half-width for a monomer [ $\text{cm}^{-1}$ ]	1050	910	912	1377	1402	1394
polymer $\lambda_{\max}^A$ [nm]	309.2	313.8	311.4	311.4	305.0	303.4
CT band half-width for a polymer [ $\text{cm}^{-1}$ ]	1402	1020	1079	1540	1485	1507
Absorbance of 1 g in 1 L of solution	32.68	39.1	45.2	31.9	27.99	9.0
fluorescence quantum yield	0.088	0.063	0.11	0.13	0.15	0.19
$\mu_g^{\text{cal}}$ (calculated) [D]	1.705	2.947	3.397	3.215	1.871	1.187

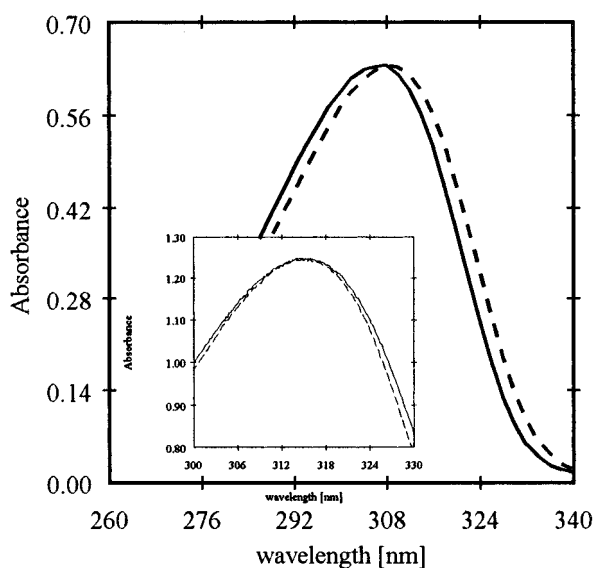


**Figure 1.** Electronic absorption spectra of a PIP molecule in THF solution: solid line, monomer model compound, broken line, polymer-bonded probe. Inset: Electronic absorption spectra of DMAB in  $\text{H}_2\text{O}$  (solid line) and a DMAB inclusion complex with  $\alpha$ -cyclodextrin.

red shift (about 2–3 nm for DMAB and DEAB) and a larger red shift of about 6–7 nm for MOR, PIP, and 26DMM.

This specific behavior can be explained by assuming that in the ground state twisting of either the donor with respect to the acceptor or vice versa can have a large impact on the resulting charge distribution. For the probes attached to the polymeric chain, the angle of the dialkylamino group with respect to the phenyl ring can differ from the angle for the free molecule. This can change the charge distribution. For the tested probe the polymeric chain can force less planar geometry causing a bathochromic shift and a broadening of the absorption band in the electronic absorption spectra. The opposite effect is observed for ethyl 4-(dimethylamino)benzoate in its inclusion complex in  $\alpha$ -cyclodextrin in water (see Figure 1, inset). Complexation causes the narrowing of the electronic absorption spectra, e.g., narrowing the distribution of the ground-state conformers. The results presented in Figure 1 as well as the calculated values of the CT band half-width, summarized in Table 1, show that the proximity of the

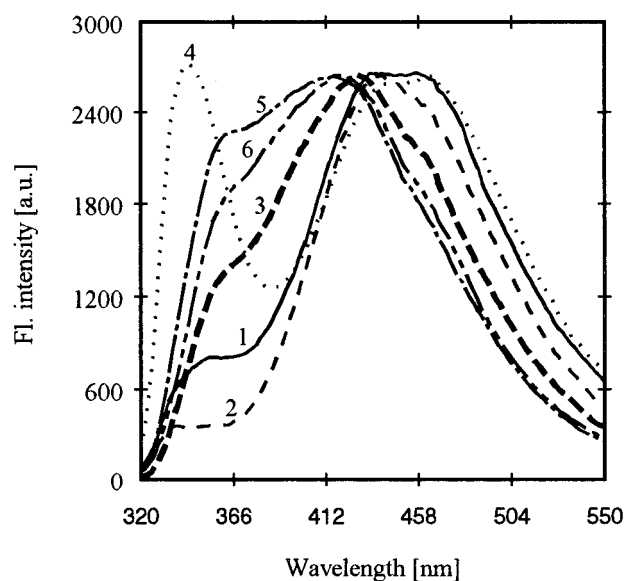


**Figure 2.** Fluorescence emission spectra of tested monomer model compounds in THF solution: (1) DMAB, (2) DEAB, (3) PYR, (4) PIP, (5) MOR, and (6) 26DMM  $\lambda_{\text{ex}} = 305$  nm.

polymeric chain leads to a broader distribution of the ground-state conformers.

The probe molecules, both free and attached to the polymeric chain, exhibit dual fluorescence. In the vicinity of 350 nm there is an emission assigned to the emission from the locally excited state (LE state; emission from the planar geometry) and the emission with  $\lambda_{\text{Fl}}^{\text{max}}$  in the vicinity of 450–520 nm which originates from the twisted intramolecular charge-transfer state (TICT state). These are shown in Figure 2.

The comparison of fluorescence spectra for free and polymer-bonded molecules demonstrates, in careful comparison, substantial dissimilarity for part of the tested probes. Figure 3 shows the comparison of the fluorescence emission spectra recorded for selected free and polymer-bonded probes in THF solution. It is easy to see that for DEAB (Figure 3, inset) the polymer chain has a rather small influence on the shape of the fluorescence spectrum. On the other hand, comparison of fluorescence spectra for MOR and PYR (Figure 3) shows an appreciable influence of the polymeric chain on the ratio of fluorescence intensities from both states ( $I_{\text{TICT}}^{\text{F}}/I_{\text{LE}}^{\text{F}}$ ).

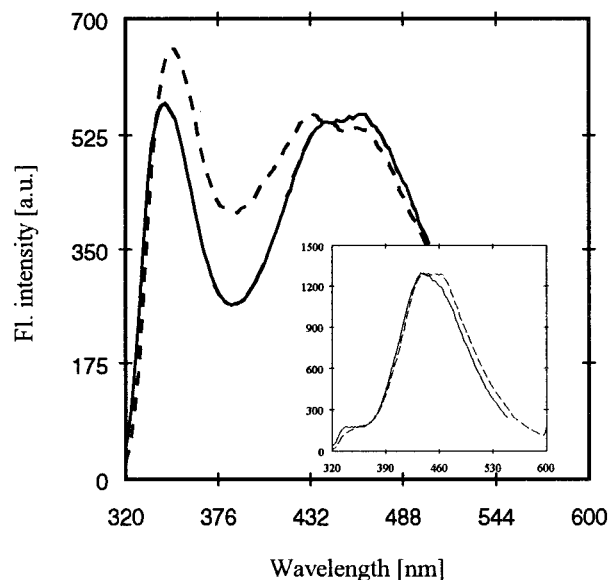


**Figure 3.** Fluorescence emission spectra of PYR chromophore in THF solution: solid line, monomer model compound; dashed line, polymer-bonded molecule  $\lambda_{\text{ex}} = 305$  nm. Inset: Fluorescence emission spectra of DEAB in THF solution  $\lambda_{\text{ex}} = 305$  nm. Red-shifted spectra for a polymer-bonded probe.

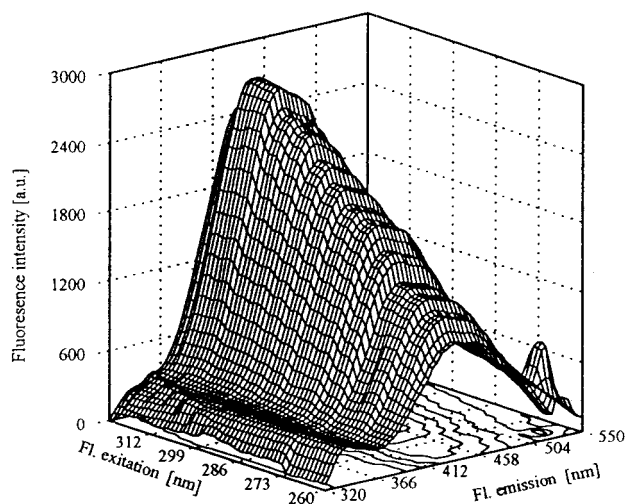


**Figure 4.** 3D fluorescence emission spectra of DEAB in THF solution.

These specific properties can be explained in part by assuming the presence of the red edge effect (REE) on the TICT fluorescence. The REE describes the excitation wavelength dependence on the fluorescence emission spectra.<sup>43–45</sup> Namely, excitation of the ground-state conformers which are already partially twisted causes absorption at the edge of absorption band, and this leads to change in the fluorescence spectrum. The larger the pretwist angle of the donor moiety of a probe, the larger the fluorescence intensity from TICT state compared with the normal fluorescence band and the larger the edge effect. For the polymeric system, this effect was described by Tazuke et al.<sup>37,38</sup> The REE is illustrated in Figure 4, which shows a 3D representation of a relationship between the spectral distribution of the fluorescence spectra and the excitation wavelength for the DEAB probe. The results show a significant influence of the excitation wavelength on the ratio of emissions from TICT and LE states. Figure 5 summarizes this behavior for all probes tested (monomer model compounds). Similar properties are observed for poly-

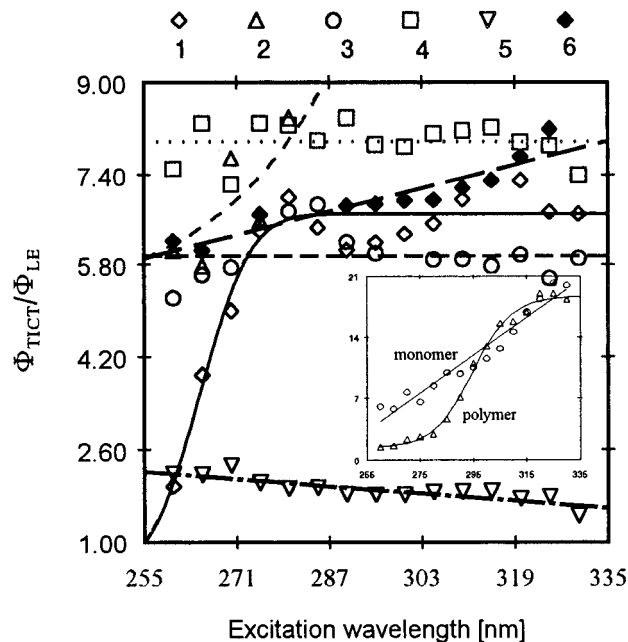
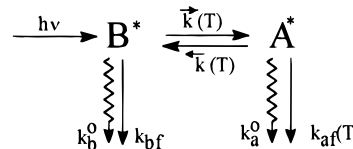


**Figure 5.** Emission intensity ratio ( $R = \Phi_{\text{TICT}}/\Phi_{\text{LE}}$ ) of tested monomer model compounds versus excitation wavelength. Solvent = THF. Inset: Emission intensity ratio ( $R = \Phi_{\text{TICT}}/\Phi_{\text{LE}}$ ) of DEAB monomer model compound (circles) and polymer-bonded chromophore (triangles) versus excitation wavelength. Solvent = THF.

### Scheme 3



meric systems. Only the DEAB molecule shows significant REE (see Figure 5, inset) for both free and polymer-bonded molecules. Experimental results show that there is (i) no polymeric chain effect on emission distribution for the DMAB molecule, (ii) significant REE for the PIP probe, (iii) slight REE for 26DMM, (iv) a specific blue edge effect for the PYR probe, and (v) a combination of REE and BEE for MOR. Analysis of the data indicates that the neighboring polymeric chain causes a magnification of the edge effects (see Figure 5, inset).

In the discussions of the intramolecular charge-transfer dynamics in medium- and high-polarity solvents, the mechanism developed by Grabowski<sup>46</sup> and represented by Scheme 3 is generally employed. The scheme formally is identical with one governing intramolecular excimer and exciplex formation<sup>47,48</sup> with three thermally activated processes.

In the TICT approach the forward and backward reactions involve an orientational relaxation of the solvent as well as structural relaxation by rotation of the alkylamino group<sup>33,34,46</sup> where  $k(T) = k^\infty \exp(-E_1/RT)$  for reaction  $\text{LE}^* \rightarrow \text{TICT}^*$ ,  $\bar{k}(T) = \bar{k}^\infty \exp(-E_2/RT)$  for reaction  $\text{TICT}^* \rightarrow \text{LE}^*$ , and TICT fluorescence  $k_{\text{af}}(T) = k_{\text{af}}^0 + k_{\text{af}}^1 \exp(-h\nu_1/c kT)$ .

The temperature dependence of the dual fluorescence of tested molecules, as shown in Figures 6 and 7, displays very characteristic features. For DMAB in the low-temperature region the short-wavelength LE band shows a slight increase of intensity as temperature

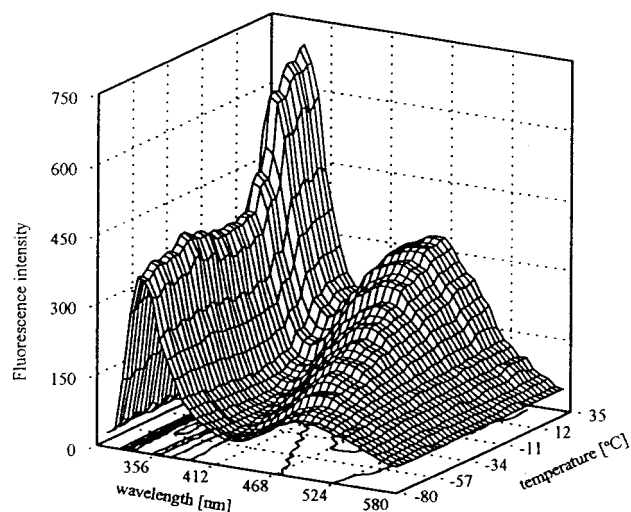


**Figure 6.** 3D presentation of fluorescence emission intensity as a function of temperature for DMAB in THF solution.  $\lambda_{\text{ex}} = 305$  nm;  $c = 0.6 \times 10^{-5}$  M.

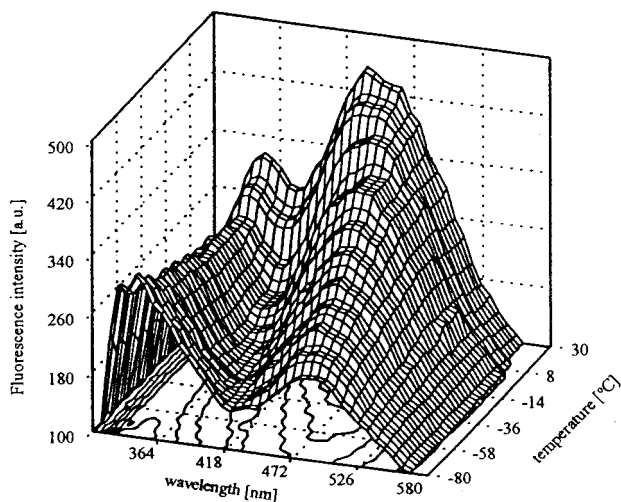


**Figure 7.** 3D presentation of the temperature dependence of the fluorescence intensity for poly-DMAB in THF solution.  $\lambda_{\text{ex}} = 305$  nm; concentration of chromophore  $c = 1 \times 10^{-5}$  M.

increase and a sharp increase at higher temperature, whereas the intensity of the TICT band increases sharply with temperature. For poly-DMAB the short-wavelength LE band has approximately a constant intensity in the whole temperature range, while the TICT fluorescence intensity increases monotonically with temperature. This specific behavior is different for each tested molecule. The temperature dependence of the fluorescence intensity ratio can be pictured by means of the kinetic scheme presented in Scheme 1.

In the general case, the kinetics of the phenomenon can be described by the two coupled equations describing the rate of formation of two emitting states. Approximations ( $\bar{k}[b^*] = k_a^0 + k_{\text{af}}^1 + k[\bar{a}^*]$  and  $I_{\text{abs}} = k_b^0[b^*] + k_{\text{af}}^1[a^*] + k_a^0[a^*]$ ) for the steady state give for the quantum yields

$$\Phi_{\text{LE}} = \frac{k_{\text{bf}}[k_a^0 + k_{\text{af}}^1 + \bar{k}]}{[k_a^0 + k_{\text{af}}^1][k_b^0 + \bar{k} + k_b^0] + k_b^0\bar{k}} \quad (1)$$

$$\Phi_{\text{TICT}} = \frac{\bar{k}[k_{\text{af}}^0 + k_{\text{af}}^1]}{[k_a^0 + k_{\text{af}}^1][k_b^0 + \bar{k}] + k_b^0\bar{k}} \quad (2)$$

and

$$\frac{\Phi_{\text{TICT}}}{\Phi_{\text{LE}}} = \frac{\bar{k}[k_{\text{af}}^0 + k_{\text{af}}^1]}{k_{\text{bf}}[k_a^0 + k_{\text{af}}^1 + \bar{k}]} \quad (3)$$

Experimental results<sup>46</sup> have shown that usually  $\bar{k} > k_b^0$ ,  $k_a^0 > k_{\text{af}}^1$ , and frequently  $k_{\text{af}}^1 > k_{\text{af}}^0$ . Under these conditions the following expression is obtained:

$$\frac{\Phi_{\text{TICT}}}{\Phi_{\text{LE}}} = \frac{k_{\text{af}}^1\bar{k}}{k_{\text{bf}}[k_a^0 + k_{\text{af}}^1 + \bar{k}]} \quad (4)$$

For the TICT chromophores the plot of  $\ln(\Phi_{\text{A}}/\Phi_{\text{B}})$  versus  $1/T$  passes a maximum ( $T_{\text{M}}$ ). For temperatures below  $T_{\text{M}}$  the backreaction  $\text{TICT} \rightarrow \text{LE}$  can be neglected against  $k_{\text{af}}^1$  because of its high activation energy  $E_2$ . According to Grabowski et al.<sup>46</sup> and Rettig,<sup>35</sup>  $k_a^0$  is much larger than  $k_{\text{af}}^1$ ; thus in the low-temperature region below  $T_{\text{M}}$ , eq 4 can be simplified to

$$R = \frac{\Phi_{\text{TICT}}}{\Phi_{\text{LE}}} = \frac{k_{\text{af}}^1\bar{k}}{k_{\text{bf}}k_a^0} \quad (5)$$

Thus, the plot of  $\ln(\Phi_{\text{A}}/\Phi_{\text{B}})$  versus  $1/T$  in the low-temperature region should give a linear relationship with a slope of  $-E_1/R - (h\nu_1/c/k)$ .  $h\nu_1c = \epsilon$  represents the energy gap between the lowest and second lowest vibrational levels of the TICT state (the fluorescence from the TICT state should be strongly forbidden,  $k_{\text{af}}^0$  is on the order of  $10^6 \text{ s}^{-1}$ ; the thermally activated emission from higher vibrational levels is less forbidden; the rate constant  $k_{\text{af}}^1$  is close to  $10^7$ – $10^8$ ).<sup>34</sup> In the high-temperature region above  $T_{\text{M}}$ , the backreaction  $\text{A}^* \rightarrow \text{B}^*$  cannot be neglected, and since under this condition  $k_{\text{af}}^0 < \bar{k}$ , eq 6 can be simplified to the form

$$R = \frac{\Phi_{\text{TICT}}}{\Phi_{\text{LE}}} = \frac{k_{\text{af}}^1\bar{k}}{k_{\text{bf}}\bar{k}} \quad (6)$$

A plot of  $\ln(\Phi_{\text{A}}/\Phi_{\text{B}})$  versus  $1/T$  in the high-temperature region should be linear with a slope of  $(E_2/R) - [(E_1/R) - h\nu_1c/k]$ .

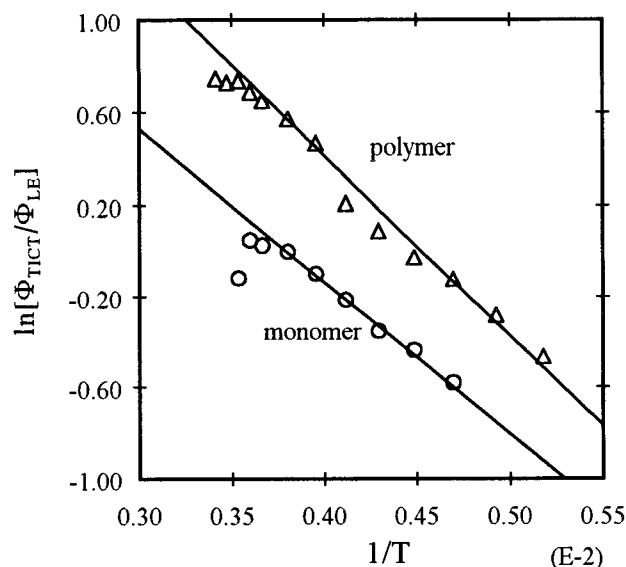
Application of eqs 5 and 6 to the experimental data allows us to evaluate the energies involved:  $E_1$ ,  $E_2$ ,  $\Delta H$ , and  $\epsilon = h\nu_1c$ . Practically, only one or two characteristic values are accessible from experimental measurements.

Figure 8 shows the temperature dependence of the quantum yields  $\Phi_{\text{TICT}}$  and  $\Phi_{\text{LE}}$  ratio for the DMAB chromophore. PYR and DEAB behave similarly, displaying the kinetic behavior predicted above.

For DMAB molecules similar properties were described by Tazuke et al.<sup>37,38</sup> However, the features of 26DMM (Figure 9) and MOR probes significantly differ from the properties presented in Figure 8. Both the free and polymer-bonded molecules show in the low-temperature region a dependence of  $\ln(\Phi_{\text{A}}/\Phi_{\text{B}})$  on  $1/T$ , with a low slope which increases with increasing temperature.

One can explain this specific behavior by assuming that the TICT state is formed with or without the crossing of an energy barrier with the activation energy  $E_1$ . This is illustrated in Scheme 4.

For a pretwisted molecule, the Franck–Condon transition can occur below and above the twist angle marked in Scheme 4 as  $Q_{\text{max}}$ . For this reason, for the discussion



**Figure 8.** Temperature dependence of the fluorescence intensity ratio ( $\Phi_{\text{TICT}}/\Phi_{\text{LE}}$ ) for DMAB monomer model compound (circle) and polymer-bonded chromophore (triangles) in THF solution.  $\lambda_{\text{ex}} = 305$  nm; chromophore concentration  $c = 1 \times 10^{-5}$  M.

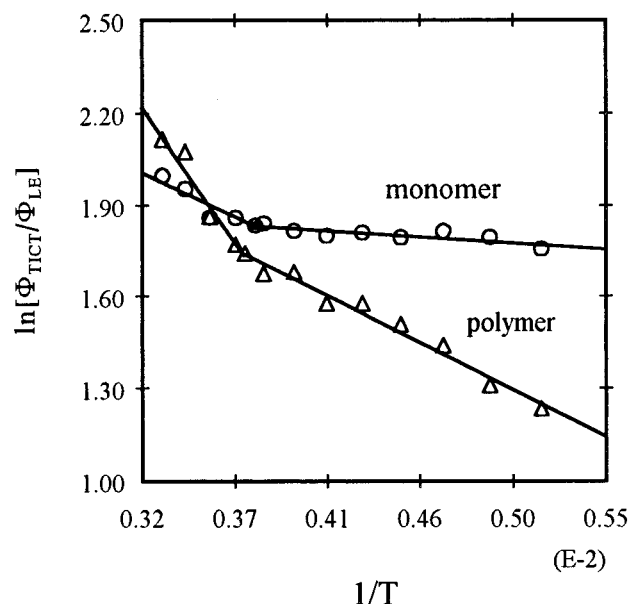


**Figure 9.** Temperature dependence of the fluorescence intensity ratio ( $\Phi_{\text{TICT}}/\Phi_{\text{LE}}$ ) for 26DMM (circles) and poly-26DMM (triangles). Solvent = THF.  $\lambda_{\text{ex}} = 305$  nm; concentration of chromophore  $c = 2 \times 10^{-5}$  M.

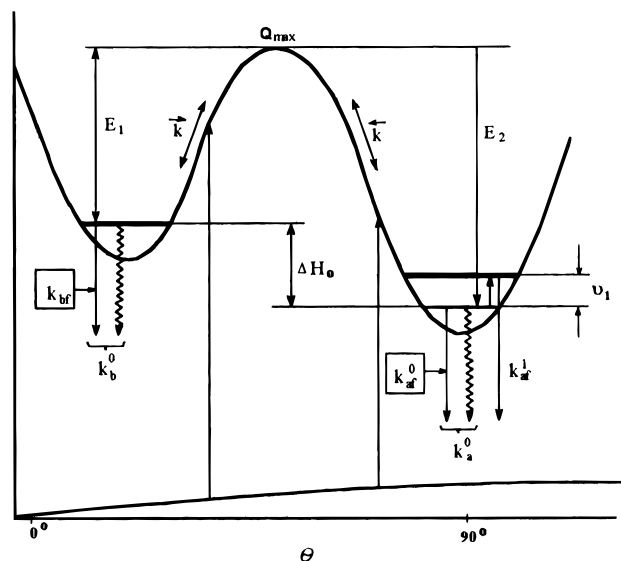
on 26DMM and MOR properties, one should apply the kinetic Scheme 5.

In order to understand and interpret the data related to the excited-state properties, it is necessary to discuss the ground-state properties of the tested molecules. According to Rettig,<sup>35</sup> the ground-state angle between the amino group and the phenol ring is different for the cyclic amines. The average angle may be followed by UV spectroscopy, assuming the validity of the  $\cos^2$  law for the absorption coefficient low  $\epsilon$ .<sup>49</sup>

$$\epsilon/\epsilon_{\text{ref}} = \cos^2 \theta \quad (7)$$

where  $\theta$  is a spectroscopic twist angle. For convenience DMAB is chosen as the reference compound, because a sterically planar reference compound is not available

**Scheme 4**



**Scheme 5**

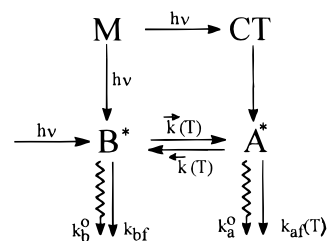


**Table 2.** Calculated Ground-State Spectroscopic Angle for Tested Molecules

	DMAB	DEAB	PYR	PIP	MOR	26DMM
$\epsilon_{\text{max}}$	33 900	31 400	32 800	24 700	23 000	17 000
$\theta$ [deg]	0	15	~10	31	34	45

and because the most probable twist angle for DMAB is closest to zero. The lower values of absorption coefficients for other tested compounds suggest somewhat twisted ground-state conformations. Table 2 summarizes the calculated (based on, e.g., ref 7) spectroscopic twist angles.

Considering the ground-state spectroscopic angle and additionally the broadening of the electronic absorption spectra caused by the polymeric chain, one can adopt Scheme 5 for the kinetic description of the observed phenomenon.

Steady-state conditions are the same as those for the kinetics represented by eqs 1–6. However, the quantum yield of the fluorescence from LE state is

$$\Phi_{\text{LE}} = \frac{k_{\text{bf}} \bar{k}}{(k_{\text{a}}^0 + k_{\text{af}}^1)(k_{\text{b}}^0 + \bar{k}) + k_{\text{b}}^0 \bar{k}} \quad (8)$$

and for the TICT state adequately

$$\Phi_{\text{TICT}} = \frac{k_{\text{af}}^1 [k_{\text{b}}^0 + \bar{k}]}{(k_{\text{a}}^0 + k_{\text{af}}^1)(k_{\text{b}}^0 + \bar{k}) + k_{\text{b}}^0 \bar{k}} \quad (9)$$

and the ratio

$$\frac{\Phi_{\text{TICT}}}{\Phi_{\text{LE}}} = \frac{k_{\text{af}}^1 [k_{\text{b}}^0 + \bar{k}]}{k_{\text{bf}} \bar{k}} \quad (10)$$

**Table 3. Photophysical Parameters of Tested Probes in THF Solution**

molecule	free			polymer			difference		
	$-E_1 - \epsilon_1$ [kJ/mol]	$-\epsilon_1$ [kJ/mol]	$H_m$ [kJ/mol]	$-E_1 - \epsilon_1$ [kJ/mol]	$-\epsilon_1$ [kJ/mol]	$H_p$ [kJ/mol]	$\Delta(-E_1 - \epsilon_1)$ [kJ/mol]	$\Delta(-\epsilon_1)$ [kJ/mol]	$\Delta H$ [kJ/mol]
DMAB	5.5			6.1				0.6 (50 cm <sup>-1</sup> )	
DEABM	6.4			7.2				0.6 (50 cm <sup>-1</sup> )	
26DMM	2.6	0.4 (30 cm <sup>-1</sup> )		8.0	2.8 (225 cm <sup>-1</sup> )		5.4	2.4 (195 cm <sup>-1</sup> )	
MORM	3.5	0.2 (15 cm <sup>-1</sup> )		8.6	2.9 (240 cm <sup>-1</sup> )		5.1	2.7 (225 cm <sup>-1</sup> )	
PIPM			3.7			2.1			1.6
PIRM			1.0		1.5 (125 cm <sup>-1</sup> )	3.4			2.4

Taking into account that usually  $\bar{k} > k_b^0$ , one obtains

$$\frac{\Phi_{\text{TICT}}}{\Phi_{\text{LE}}} = \frac{k_{\text{af}}^1 \bar{k}}{k_{\text{bf}} \bar{k}} \quad (11)$$

For low temperature, the TICT formation from the LE state and the backreaction TICT  $\rightarrow$  LE can be neglected against  $k_{\text{af}}^1$  because of their high activation energies,  $E_1$  and  $E_2$ . Thus, in the low-temperature region, eq 11 can be simplified to the form:

$$R = \frac{\Phi_{\text{TICT}}}{\Phi_{\text{LE}}} = \frac{k_{\text{af}}^1}{k_{\text{bf}}} \quad (12)$$

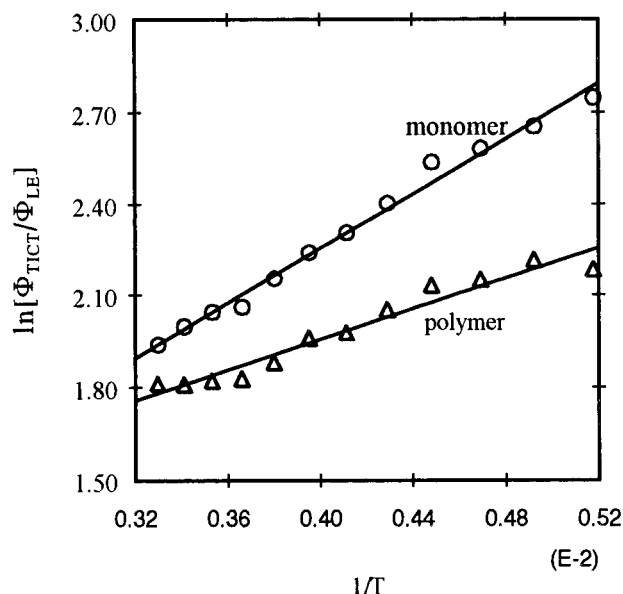
The plot of  $\ln(\Phi_{\text{TICT}}/\Phi_{\text{LE}})$  versus  $1/T$  in the low-temperature region should be linear with a slope of  $-h\nu_1/c/k$ . From the data in Figure 9 (26DMM), one can calculate appropriate activation energies. In the low-temperature region the slope corresponds to the value of energy equal to about  $-h\nu_1/c = 30 \text{ cm}^{-1}$  ( $\pm 20\%$ ) for the free molecule and about  $-h\nu_1/c = 225 \text{ cm}^{-1}$  ( $\pm 10\%$ ) for the molecule attached to the polymeric chain. For the MOR molecule the corresponding values are  $15 \text{ cm}^{-1}$  ( $\pm 20\%$ ) and  $240 \text{ cm}^{-1}$  ( $\pm 10\%$ ), respectively. According to Rettig,<sup>35</sup> the activation energy for the thermally activated TICT fluorescence for similar types of molecules (*p*-cyanodi-alkylanilines) oscillates between 95 and  $240 \text{ cm}^{-1}$ . Values calculated in this work are in the same order.

From Figure 9, for temperature close to the  $T_M$  region, one can see a distinct increase of the slope for the  $\ln(\Phi_A/\Phi_B)$  versus  $1/T$  relationship. In this region the backreaction TICT  $\rightarrow$  LE is still neglected against  $k_{\text{af}}^1$  but the formation of TICT from LE can occur. Under this approximation the relationship  $\Phi_{\text{TICT}}/\Phi_{\text{LE}} = f(1/T)$  is governed by the equation

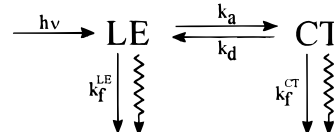
$$\frac{\Phi_A}{\Phi_B} = \frac{k_{\text{af}}^1 \bar{k}}{k_{\text{bf}}} \quad (13)$$

and the slope of the relationship  $\ln(\Phi_{\text{TICT}}/\Phi_{\text{LE}}) = f(1/T)$  includes both the activation energy of TICT state formation and the activation energy of the thermally activated fluorescence. The difference between observed slopes in the high-temperature and low-temperature regions gives the activation energy of the TICT state formation.

Specific also are the properties of the PIP (Figure 10) molecule. This may be interpreted by Zachariasse's<sup>39,40</sup> scheme for double fluorescence (Scheme 6) where  $k_a$  and  $k_d$  are the rate constants of the forward and backward charge-transfer reactions, respectively. This assumes an orientational relaxation of the solvent molecules following changes in the charge distribution of the solute



**Figure 10.** Temperature dependence of the fluorescence intensity ratio ( $\Phi_{\text{TICT}}/\Phi_{\text{LE}}$ ) for PIP (circles) and poly-PIP (triangles). Solvent = THF.  $\lambda_{\text{ex}} = 305 \text{ nm}$ ; concentration of chromophore  $c = 1 \times 10^{-5} \text{ M}$ .

**Scheme 6**

and that no structural relaxation by rotation of the amino group is involved. From an Arrhenius plot of the CT-LE fluorescence intensity ratio, one can calculate the  $-\Delta H/R$  value for the CT state stabilization enthalpy ( $\Delta H$  of about  $-3.7 \text{ kJ mol}^{-1}$  for the free molecule and about  $-2.0 \text{ kJ mol}^{-1}$  for the polymer-bonded probe, respectively). All effects discussed above are summarized in Table 3. Several major features can be deduced from the data presented in Figures 8–10 and Table 3. The most important conclusion is that the polymeric chain essentially does not change the activation energy for the thermally activated TICT state formation. Rettig's study<sup>35</sup> has shown that the rate determining step for the formation of the emitting TICT species is governed by viscosity effects. The absence of an influence of the polymeric chain on  $E_1$  indicates that the polymeric chain does not change the microscopic viscosity in the range affecting measurable changing of the TICT-LE equilibrium. On the other hand, from the presented data one can conclude that the polymeric chain increases the energetic gap between the lowest forbidden  $\nu_0$  vibrational state and the less forbidden  $\nu_1$  vibrational state. The increase of the energy gap between these two states is on the order of  $195\text{--}225 \text{ cm}^{-1}$  ( $0.6\text{--}2.4 \text{ kJ mol}^{-1}$ ). This specific behavior can be



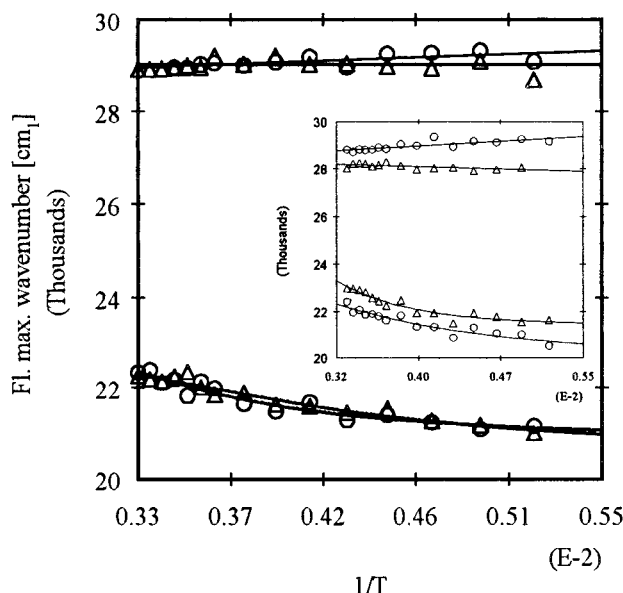


**Figure 11.** Fluorescence emission maximum wavenumber as a function of temperature for DEAB (circles) and poly-DEAB (triangles). Solvent = THF.  $\lambda_{\text{ex}} = 305$  nm; concentration of chromophore  $c = 1 \times 10^{-5}$  M. Inset: Fluorescence emission maximum wavenumber as a function of temperature for MOR (circles) and poly-MOR (triangles). Solvent = THF.  $\lambda_{\text{ex}} = 305$  nm; concentration of chromophore  $c = 1 \times 10^{-5}$  M.

explained by assuming that the polymeric chain affects only the vibrational relaxation of tested molecules and does not influence the thermodynamics of the TICT and LE state equilibrium. This supposition might be supported by one more interesting feature deduced from the fluorescence intensity ratio. From the ordinate obtained for the linear relationship between  $\ln(\Phi_{\text{TICT}}/\Phi_{\text{LE}})$  versus  $1/T$ , it is easy to conclude that, for molecules following Grabowski's kinetic model, the  $k_{\text{bf}}$  value is decreasing (higher ordinate) for the polymeric system. This observation suggests that the neighboring polymeric chain stabilizes the emitting state of the molecules.

One observes a specific relationship when the TICT state fluorescence  $\lambda_{\text{max}}$  is plotted against  $1/T$ . These properties are illustrated in Figure 11. Figure 11 shows that the MOR chromophore (PYR behaves similarly) shows a distinct red shift of the TICT state emission when temperature is decreasing. On the other hand, for DEAB (26DMM behaves similarly) there are no significant fluorescence  $\lambda_{\text{max}}$  shifts at any temperatures investigated (see Figure 11, inset). There are several possible explanations of the phenomenon. One of them is that the solvent reorientation is slow as compared to the lifetime of the polar TICT state. Another possible explanation is that a change of the number of solvent molecules in the first solvent shell is involved.

For the polymeric system, fewer molecules (less than in the case of pure solvent) are interacting with the solute dipole. This may cause a difference between the spectroscopic properties of the free and polymer-bonded probe molecules. This interpretation is in good agreement with the results obtained for DMAB, DEAB, PIP, and 26DMM probes.

**Acknowledgment.** This research was sponsored by the State Committee for Scientific Research (KBN) (Grants BS7/93 and BW21/93).

## References and Notes

- (1) Loutfy, R. O. *Macromolecules* **1981**, *14*, 270; *J. Polym. Sci., Polym. Phys. Ed.* **1982**, *20*, 825; *Pure Appl. Chem.* **1986**, *58*, 1239.
- (2) Cho, D.; Mattice, W. L.; Porter, L. J.; Hemingway, R. W. *Polymer* **1989**, *30*, 1955.
- (3) Kamat, P. V.; Gupta, S. K. *Polymer* **1988**, *29*, 1329.
- (4) Kamat, P. V. *Anal. Chem.* **1987**, *59*, 1636.
- (5) Van Ramesdonk, H. J.; Vos, M.; Verhoven, J.; Mohlman, G. R.; Tissink, N. A.; Meesen, A. W. *Polymer* **1987**, *28*, 951.
- (6) Jenneskens, L. W.; Verhey, H. J.; Van Ramesdonk, H. J.; Witteveen, A. J.; Verhoven, J. W. *Macromolecules* **1991**, *24*, 4038.
- (7) Small, R. D.; Ors, J. A.; Royle, B. S. *ACS Symp. Ser.* **1984**, *242*, 325.
- (8) Klosterboer, J. G.; Van de Hei, G. M. M.; Gossink, R. G.; Dorant, G. C. M. *Polym. Commun.* **1984**, *25*, 322.
- (9) Wang, F. W.; Lowry, R. E.; Grant, W. H. *Polymer* **1984**, *25*, 690.
- (10) Wang, F. W.; Lowry, R. E.; Cavanagh, R. *Polymer* **1985**, *26*, 1657.
- (11) Wang, F. W.; Lowry, R. E.; Fanconi, B. M. *Polymer* **1986**, *27*, 1529.
- (12) Nishijima, Y.; Mito, Y. *Rep. Prog. Polym. Phys. Jpn.* **1967**, *10*, 139.
- (13) Nishijima, Y. *J. Polym. Sci., Part C* **1970**, *31*, 353.
- (14) Onsager, L. *J. Am. Chem. Soc.* **1936**, *58*, 1486.
- (15) Pączkowski, J.; Neckers, D. C. *Macromolecules* **1992**, *25*, 548.
- (16) Lin, K.-F.; Wang, F. W. *Polymer* **1994**, *35*, 687.
- (17) Pączkowski, J.; Neckers, D. C. *Chemtracts: Macromol. Chem.* **1992**, *3*, 75.
- (18) Morawetz, H. *J. Lumin.* **1989**, *43*, 59.
- (19) Holden, D. A.; Guillet, J. E. *Developments in Polymer Photochemistry*; Applied Science Publishers Ltd.: London, 1980; Vol. 1, Chapter 2, pp 27–68.
- (20) Guillet, J. *Polymer Photophysics and Photochemistry*; Cambridge University Press: Cambridge, U.K., 1985.
- (21) Lippert, E. *Z. Naturforsch.* **1955**, *10A*, 541; *Z. Electrochem.* **1957**, *61*, 962.
- (22) Mataga, N.; Kaifu, Y.; Koizumi, M. *Bull. Chem. Soc. Jpn.* **1957**, *29*, 962.
- (23) Bilot, L.; Kowski, A. *Z. Naturforsch.* **1962**, *17A*, 621.
- (24) Kowski, A. *Acta Phys. Pol.* **1966**, *29*, 507.
- (25) Abdel-Mottabed, M. S. A.; Loutfy, R. O.; Lapouyade, R. *J. Photochem. Photobiol.* **1989**, *48*, 87.
- (26) Hermant, R. M. *Highly Fluorescent Donor–Acceptor Systems; Fundamentals and Applications*. Thesis, Department of Organic Chemistry, University of Amsterdam, 1990.
- (27) Pączkowski, J.; Neckers, D. C. *J. Photochem. Photobiol., A* **1991**, *62*, 173.
- (28) Safarzadek-Amri, A.; Thompson, M.; Krull, U. *J. Photochem. Photobiol.* **1989**, *48*, 87.
- (29) Lippert, E.; Lüder, W.; Moll, F.; Nägele, W.; Boss, H.; Prigge, H.; Seibold-Blankenstein, I. *Angew. Chem.* **1961**, *73*, 695.
- (30) Lippert, E.; Lüder, W.; Boos, H. *Advances in Molecular Spectroscopy*; Mangini, A., Ed.; Pergamon Press: Oxford, U.K., 1962; Vol. 1, p 443.
- (31) Lippert, E. *Organic Molecular Photophysics*; Birks, J. B. Ed.; Wiley-Interscience: New York, 1975; Vol. 2, p 1.
- (32) Wermuth, G.; Rettig, W.; Lippert, E. *Ber. Bunsen-Ges. Phys. Chem.* **1981**, *85*, 64.
- (33) Rotkiewicz, K.; Grellmann, K. H.; Grabowski, Z. R. *Chem. Phys. Lett.* **1973**, *19*, 315.
- (34) Grabowski, Z. R.; Rotkiewicz, K.; Siemiarczuk, A.; Cowley, D.; Baumann, W. *Nouv. J. Chim.* **1979**, *2*, 443.
- (35) Rettig, W. *J. Lumin.* **1980**, *26*, 21.
- (36) Rettig, W. *J. Phys. Chem.* **1982**, *86*, 1970.
- (37) Hayashi, R.; Tazuke, S.; Frank, C. W. *Chem. Phys. Lett.* **1987**, *135*, 123; *Macromolecules* **1987**, *20*, 123.
- (38) Tazuke, S.; Kun Guo, R.; Hayashi, R. *Macromolecules* **1988**, *21*, 1046; *Macromolecules* **1989**, *22*, 729.
- (39) Leinhos, U.; Khnle, W.; Zachariasse, K. A. *J. Phys. Chem.* **1991**, *95*, 2013.
- (40) Schuddeboom, W.; Jonker, S. A.; Warman, J. M.; Leinhos, U.; Khnle, W.; Zachariasse, K. A. *J. Phys. Chem.* **1992**, *96*, 10809.

- (41) Pączkowski, J.; Bajorek, A.; Wencel, K.; Sierocka, M. *Polimery*, **1992**, 37, 825.
- (42) Shur, H. *Ann.* **1965**, 687.
- (43) Al-Hassan, K. A.; El-Bayoumi, M. A. *Chem. Phys. Lett.* **1980**, 76, 121.
- (44) Al-Hassan, K. A.; Azumi, T. *Chem. Phys. Lett.* **1989**, 163, 129.
- (45) Al-Hassan, K. A.; Azumi, T.; Rettig, W. *Chem. Phys. Lett.* **1993**, 206, 25.
- (46) Grabowski, Z. R.; Rotkiewicz, K.; Rubaszewska, W.; Kirkor-Kamińska, E. *Acta Phys. Pol.* **1978**, A54, 767.
- (47) Birks, J. B. *Photophysics of Aromatic Molecules*; Wiley-Interscience: New York, 1970.
- (48) Birks, J. B. *Nouv. J. Chim.* **1977**, 1, 453.
- (49) Wepster, B. M. *Rec. Trav. Chim. Pays-Bas* **1957**, 76, 335.

MA970378Q